Therapeutics, Targets, and Chemical Biology

Cancer Research

Sodium Orthovanadate Inhibits p53-Mediated Apoptosis

Akinori Morita[1], Shinichi Yamamoto[1], Bing Wang[3], Kaoru Tanaka[3], Norio Suzuki[4], Shin Aoki[5], Azusa Ito[1], Tomohisa Nanao[1], Soichiro Ohya[1], Minako Yoshino[1], Jin Zhu[6], Atsushi Enomoto[6], Yoshihisa Matsumoto[6], Osamu Funatsu[2], Yoshio Hosoi[6], and Masahiko Ikekita[1,2]

Abstract

Sodium orthovanadate (vanadate) inhibits the DNA-binding activity of p53, but its precise effects on p53 function have not been examined. Here, we show that vanadate exerts a potent antiapoptotic activity through both transcription-dependent and transcription-independent mechanisms relative to other p53 inhibitors, including pifithrin (PFT) α. We compared the effects of vanadate to PFTα and PFTμ, an inhibitor of transcription-independent apoptosis by p53. Vanadate suppressed p53-associated apoptotic events at the mitochondria, including the loss of mitochondrial membrane potential, the conformational change of Bax and Bak, the mitochondrial translocation of p53, and the interaction of p53 with Bcl-2. Similarly, vanadate suppressed the apoptosis-inducing activity of a mitochondrially targeted temperature-sensitive p53 in stable transfectants of SaOS-2 cells. In radioprotection assays, which rely on p53, vanadate completely protected mice from a sublethal dose of 8 Gy and partially from a lethal dose of 12 Gy. Together, our findings indicated that vanadate effectively suppresses p53-mediated apoptosis by both transcription-dependent and transcription-independent pathways, and suggested that both pathways must be inhibited to completely block p53-mediated apoptosis. *Cancer Res; 70(1); 257–65. ©2010 AACR.*

Introduction

Acute radiation lethality is largely caused by the injury of particularly sensitive organs, the bone marrow and gastrointestinal tract; these injuries are known as hematopoietic syndrome and gastrointestinal syndrome, respectively (1). In these organs, genotoxic stress induces massive apoptosis, which causes some of the adverse side effects of anticancer radiation therapy and chemotherapy that frequently restrict their use (2). To overcome this dose-limiting toxicity, free-radical scavengers containing an antioxidant moiety such as a thiophosphate group were developed as radioprotectors (1, 3). More recently, new radioprotectors that inhibit apoptosis have been introduced. These drugs are intended to minimize the apoptosis-inducing sensitivity of target organs. They inhibit proapoptotic components or activate antiapoptotic ones; for example, they inhibit the proapoptotic functions of p53 (4–6), mimic the antiapoptotic Bcl-2 family proteins (7), or enhance antiapoptotic pathway(s) by activating the Toll-like receptor 5 signal (8).

Although the molecules responsible for the radiation sensitivity of target organs have not been fully identified, p53 is a well-known culprit and is considered a good target for therapeutic radioprotection. In fact, mice in which p53 function has been genetically inhibited show increased resistance to genotoxic stress from radiation (5, 9). Five chemical p53 inhibitors have been reported: pifithrin (PFT) α (4, 5), PFTμ (6), sodium salicylate (10), cadmium chloride (11), and sodium orthovanadate (vanadate; ref. 12). At present, the radioprotective efficacy of only PFTα and PFTμ has been shown in mice (4–6). All of the inhibitors, except PFTμ, block transcriptional changes induced by p53, albeit in slightly different manners.

PFTμ, on the other hand, uniquely inhibits the mitochondrial branch of the p53 apoptotic pathway, called the "transcription-independent pathway." This pathway is activated by a direct interaction between stress-activated p53 and mitochondrial Bcl-2 family members, including Bcl-2, Bcl-xL, and Bak, resulting in the release of cytochrome *c* from the mitochondria into the cytosol (13–17). PFTμ suppresses this pathway by reducing the affinity of p53 for Bcl-2 and Bcl-xL, thereby inhibiting the binding of p53 to mitochondria, but it has little effect on the transcriptional activity of p53 (6).

The available evidence suggested that inhibiting both p53 pathways would offer the most effective radioprotection from p53-induced apoptosis. Interestingly, although PFTα mainly inhibits the transcriptional activity of p53 (18, 19), both PFTα and PFTμ protect mice from radiation

Authors' Affiliations: [1]Department of Applied Biological Science, Faculty of Science and Technology and [2]Genome and Drug Research Center, Tokyo University of Science; [3]Research Center for Radiation Protection, National Institute of Radiological Sciences, Chiba, Japan and [4]University of Tokyo; [5]Department of Radiological Health and [6]Laboratory of Molecular Radiology, Center for Disease Biology and Integrative Medicine, Graduate School of Medicine, University of Tokyo, Tokyo, Japan

Note: Supplementary data for this article are available at Cancer Research Online (http://cancerres.aacrjournals.org/).

A. Morita and S. Yamamoto contributed equally to this work.

Corresponding Authors: Masahiko Ikekita or Akinori Morita, Department of Applied Biological Science, Faculty of Science and Technology, Tokyo University of Science, 2641 Yamazaki, Noda, Chiba 278-8510, Japan. Phone: 81-4-7122-9411; Fax: 81-4-7123-9767; E-mail: masalab@rs.noda.tus.ac.jp or morita@rs.noda.tus.ac.jp.

doi: 10.1158/0008-5472.CAN-08-3771

lethality due to hematopoietic but not gastrointestinal syndrome (5, 6). Their limited efficacy may be explained by their restricted, although different, spectra of anti-p53 activities.

Here, we initially found that vanadate had a more potent antiapoptotic activity than the other three known transcriptional inhibitors of p53. We then sought to clarify how vanadate exerted such potent protective effects, speculating that vanadate suppressed both the transcription-dependent and transcription-independent pathways. Therefore, we focused on the transcription-independent pathway and compared the effects of vanadate with those of PFTα and PFTμ. We concluded that vanadate indeed suppresses the transcription-independent pathway as well as the transcription-dependent one and that it is a potent radioprotective agent against both gastrointestinal and hematopoietic syndrome.

Materials and Methods

Cell culture and treatment. MOLT-4 cells and their derivatives were cultured in RPMI 1640 medium (Wako) supplemented with 10% fetal bovine serum (FBS; Life Technologies). SaOS-2 cells and their derivatives were cultured in DMEM/F12 medium (Wako) supplemented with 10% FBS. The medium was supplemented with 0.25 mg/mL G418 to maintain the stable transfectants. To generate the MOLT-4 transfectant harboring a p53-responsive firefly luciferase reporter (MOLT/p53-Luc1), MOLT-4 cells were cotransfected by electroporation (Gene Pulsar II, Bio-Rad) with p53-Luc plasmid (Stratagene) and a neomycin resistance gene vector (pcDNA3.1, Invitrogen). To generate SaOS-2 stable transfectants expressing temperature-sensitive (ts) p53, SaOS-2 cells were transfected with *Bgl*II-linearized ts p53 vector or mock vector [pUSEamp(+)] using FuGENE HD transfection reagent (Roche). Cells were maintained at 37°C, except for the SaOS-2 ts transfectants, which were maintained at 39°C.

Irradiation (IR) was performed at room temperature with a ^{137}Cs γ-ray source (Gammacell 40, Nordion International) at 0.83 Gy/min. Vanadate (Wako), PFTα (Alexis), and PFTμ (Calbiochem) were added to the culture medium immediately after IR unless otherwise specified. The luciferase activity was determined using the Luciferase Assay System (Promega). Semiquantitative reverse transcription-PCR (RT-PCR) was performed as described previously (12).

Flow cytometric analysis. For each sample, 10,000 cells were analyzed with a flow cytometer (FACSCalibur, Becton Dickinson). The percentage of apoptosis was determined by Annexin V-FITC staining using a MEBCYTO Apoptosis kit (MBL). The percentage of cells losing their mitochondrial membrane potential ($\Delta\psi$m) and the conformational change of Bax were measured, respectively, by MitoTracker staining and immunofluorescence staining with an anti-Bax monoclonal antibody (clone 4F11, MBL), as described previously (12). The conformational change of Bak was measured with an anti-Bak polyclonal antibody (Bak-NT, Upstate) using the same method as for the Bax staining with slight modifications: normal goat serum (Dako) was used as the blocking reagent, and FITC-labeled anti-rabbit IgG (Zymed Laboratories) was used as the secondary antibody.

Immunoblotting analysis. We used the following antibodies: p53 (clone DO-1, Santa Cruz Biotechnology), PUMA (Ab-1, Calbiochem), β-actin (clone AC-15, Sigma), Bax (clone 4F11), Bak (Bak-NT, Upstate), Bcl-2 (clone Bcl-2/100, Santa Cruz Biotechnology), VDAC1 (ab15895, Abcam), Calnexin (Stressgen), Apaf-1 (clone 24, BD Transduction Laboratories), cleaved caspase-3 (Asp^{175}, Cell Signaling), caspase-7 (clone 4G2, MBL), p21 (clone EA10, Calbiochem), or MDM2 (1:1 mixture of clone IF2 and 2A10, Calbiochem). To avoid cross-reaction between the peroxidase-conjugated secondary antibodies and immunoprecipitated immunoglobulins, the anti-p53 and anti–Bcl-2 antibodies were purchased in the peroxidase-conjugated form and used for direct detection.

Subcellular fractionation. Subcellular fractions were prepared as described by Leu and colleagues (16). Because the mitochondrial fractions also contained endoplasmic reticulum (ER), the mitochondrial and cytosolic fractions are referred to as fraction 1 and fraction 2, respectively. The protein concentrations of all the samples were determined using the bicinchoninic acid protein assay reagent (Pierce) and equalized.

Immunoprecipitation. Immunoprecipitation was performed as described previously (12). We used anti-p53 DO-1–conjugated agarose (Calbiochem), anti–Bcl-2 (7/Bcl-2, BD Transduction Laboratories), and normal mouse IgG as a negative control (Santa Cruz Biotechnology).

Vector construction. The mitochondrially targeted p53s were constructed essentially as described by Marchenko and colleagues (13), which were ligated into the *Hin*dIII/*Kpn*I site of the pUSEamp(+) vector. To generate NH_2-terminal fusion proteins with the mitochondrial import leader peptide from human ornithine transcarbamylase, a 37-codon–spanning sequence was obtained by PCR using HEK293T genomic DNA as a template, and the product was ligated to FLAG-tagged p53 by the overlap extension method (20). Because p53 has a polymorphism at amino acid 72, which can be either Pro or Arg, of which Arg confers a greater apoptotic activity (21), the Pro^{72} of each p53 (CCC) was converted to Arg (CGC). The Ala^{138} of each p53 (GCC) was converted to Val (GTC) to generate the temperature sensitivity of ts p53. The additional NH_2-terminal amino acid sequences were as follows: FLAG-tagged p53 (Np53), MDYKDDDDKL; OTC-FLAG–tagged p53 (Lp53), MLFNLRILLNNAAFRNGHNFMVRNFRCGQPLQNKVQLDYKDDDDKL.

Total body IR. Imprinting control region (ICR) female mice (SLC, Inc.), aged 8 wk, were irradiated with an X-ray generator (Pantak-320S, Shimadzu) operated at 200 kV to 20 mA at a dose rate of 0.66 Gy/min. Vanadate and a cyclic derivative of PFTα (cPFTα) were purchased from Aldrich and Calbiochem, respectively. All experimental protocols involving mice were reviewed and approved by the Animal Care and Use Committee of the National Institute of Radiological Sciences (NIRS) and performed in strict accordance with the NIRS Guidelines for the Care and Use of Laboratory Animals.

Results

The potent antiapoptotic activity of vanadate is qualitatively different from that of other p53 inhibitors. To assess the transcriptional activity of p53 *in situ*, and because MOLT-4 cells have a low transfection efficiency, we generated a MOLT-4 stable transfectant expressing a p53-responsive firefly luciferase reporter (MOLT/p53-Luc1). The luciferase activity in the MOLT/p53-Luc1 cells reached its maximum 6 hours after 10 Gy IR (Fig. 1*A* and *B*), quite similar to the transactivation kinetics of the p53 target genes in the parental MOLT-4 cells after IR (12). We also examined PUMA induction as a marker for the apoptosis-related transactivation of p53. As expected, all four p53 transactivation inhibitors suppressed the transcriptional activity of p53 and the induction of PUMA (Fig. 2*A*; Supplementary Fig. S1*A*).

Micromolar PFTα was recently reported to inhibit firefly luciferase activity (22), potentially obscuring the transcriptional activity of p53 by this measurement. However, we obtained a good correlation between the luciferase activity and the induction of PUMA, indicating that the cellular concentration of PFTα required to inhibit the transcriptional activity of p53 was less than that required to inhibit luciferase.

We also examined the effect of the inhibitors on the accumulation of p53. PFTα and salicylate suppressed the accumulation of p53, but the others did not (Fig. 2*A*; Supplementary Fig. S1*A*). We observed a slight suppression of p53 accumulation with 50 μmol/L PFTα, consistent with a previous report (4), but the induction of PUMA was completely blocked (Fig. 2*A*). Therefore, although we found that using PFTα at its saturation concentration (80 μmol/L) almost completely blocked p53 accumulation, 50 μmol/L seemed sufficient to inhibit p53-dependent transcription.

We next investigated the effects of the four inhibitors on the radiation-induced apoptosis of MOLT/p53-Luc1 cells (Fig. 2*B*; Supplementary Fig. S1*B*). In agreement with our previous study, which used the parental MOLT-4 cells (12), 800 μmol/L vanadate effectively suppressed apoptosis; however, neither PFTα nor salicylate suppressed it despite their suppression of the transcriptional activity of p53 (Fig. 2; Supplementary Fig. S1). We also examined cPFTα (23) and found that its effects were virtually the same as those of PFTα (data not shown). Although 40 μmol/L cadmium moderately suppressed apoptosis, it was cytotoxic at this and higher concentrations, and its antiapoptotic activity disappeared at 60 μmol/L. Together, these results show that the radiation-induced apoptosis in MOLT/p53-Luc1 cells did not depend entirely on the transcriptional activity of p53, and therefore, the antiapoptotic activity of vanadate was due, at least in part, to some other effect.

Because the effects of all the inhibitors tested were virtually identical in the parental and reporter cells (data not shown), we used the parental MOLT-4 cells in the following experiments to avoid any potential side effects from G418, which was used to maintain the reporter cells.

Vanadate suppresses p53-dependent DNA damage–induced apoptosis. We previously used a genetic approach to show that the suppression of DNA damage–induced apoptosis by vanadate was specifically mediated by p53 (12). Here, we confirmed and characterized the effects of vanadate on p53-induced apoptosis by using several cell systems with defective or impaired p53 function: p53-knockdown MOLT-4 transfectants expressing p53 small interfering RNA (MOLT/p53KD-1 and MOLT/p53KD-2; ref. 12), MOLT-4 transfectants (MOLT/E6-1, MOLT/E6-2, and MOLT/E6-3) expressing HPV18-E6 (an inhibitor of p53 expression; ref. 24), thymocytes from *Trp53*$^{-/-}$ mice, and p53-mutated leukemia cell lines, which all have mutation(s) in the core domain of p53 (Supplementary Fig. S2; refs. 25–27). All the data we obtained strongly suggested that the suppression of DNA damage–induced apoptosis by vanadate was specifically affected through p53, and suggested that the loss of p53 function enhanced the cytotoxic side effect(s) of vanadate.

We also investigated whether some unknown factor was involved in the effects of vanadate. First, we examined the antiapoptotic effect in MOLT-4 cells of several known phosphatase inhibitors. However, these inhibitors did not suppress the MOLT-4 apoptosis at any of the concentrations tested (Supplementary Fig. S3*A*). These findings, along with our similar results with protein tyrosine phosphatase inhibitors (12), indicated that the suppression of apoptosis by vanadate was unlikely to be through its phosphatase-inhibiting activity.

We also found that the phosphorylation of Akt, a known antiapoptotic signal relayed through phosphatidylinositol 3-kinase (PI3K) and DNA-dependent protein kinase (28), is increased by vanadate; however, the PI3K inhibitor

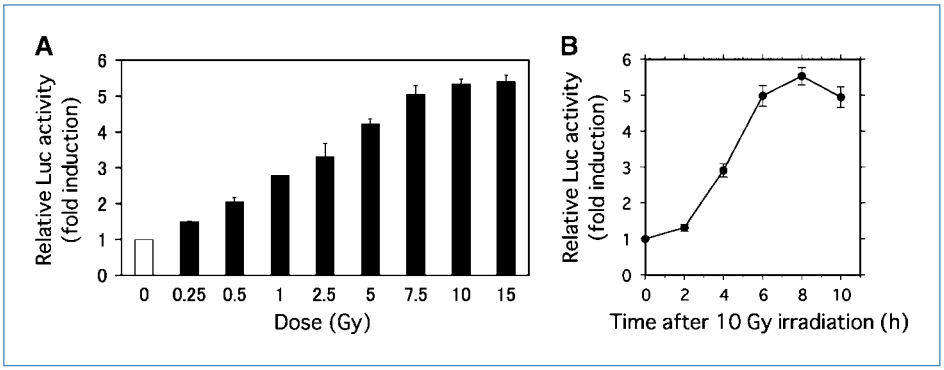

Figure 1. Analysis of the transcriptional activity of p53 in irradiated MOLT/p53-Luc1 cells. *A,* radiation dose dependency of the transcriptional activity of p53 (6 h after IR). *Columns,* mean ($n \geq 3$); *bars,* SD. *B,* time course of the transcriptional activity of p53 after 10 Gy IR. *Points,* mean ($n \geq 3$); *bars,* SD.

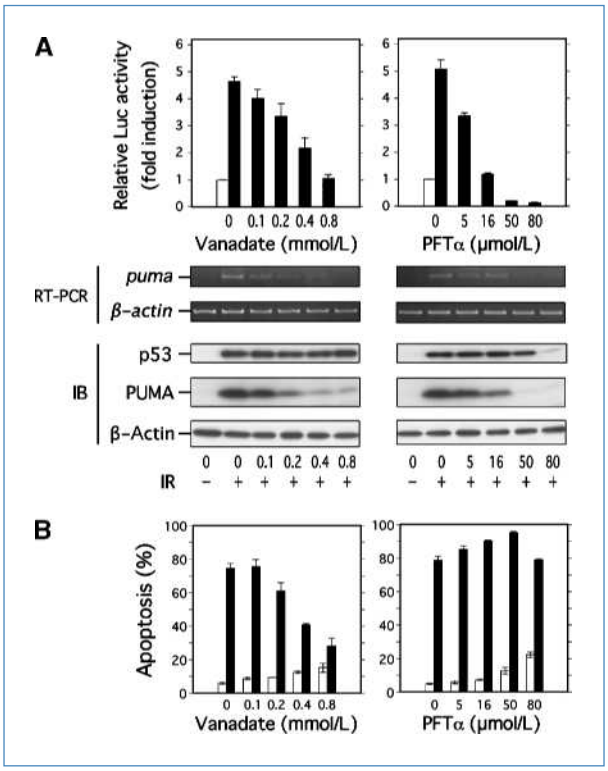

Figure 2. Effects of p53 inhibitors on the transcriptional activity and accumulation of p53, transactivation of p53 target genes, and p53-dependent apoptosis in irradiated MOLT/p53-Luc1 cells. *A,* dose dependency of the suppressive effects of p53 inhibitors on the transcriptional activity and accumulation of p53, and the induction of the p53 target gene product, PUMA (6 h after 10 Gy IR). *White columns,* unirradiated samples; *black columns,* 10 Gy–irradiated samples. *Columns,* mean ($n \geq 3$); *bars,* SD. *Bottom,* mRNAs and proteins detected by RT-PCR and immunoblotting (*IB*), respectively. *B,* dose dependency of the suppressive effects of p53 inhibitors on p53-dependent apoptosis in 10 Gy–irradiated cells. Apoptotic cells were quantified by Annexin V-FITC staining and flow cytometry. *White columns,* unirradiated samples 18 h after treatment; *black columns,* 10 Gy–irradiated samples 18 h after treatment. *Columns,* mean ($n \geq 3$); *bars,* SD.

LY294002 had little effect on the suppression of apoptosis by vanadate even when Akt phosphorylation had been reduced below that of the untreated control (Supplementary Fig. S3*B*). Thus, the upregulation of Akt phosphorylation by vanadate seems to be unrelated to its suppression of apoptosis. We also expressed the constitutively activated myr-Akt1, but it did not increase the resistance of the cells to IR and completely abolished the effects of vanadate (Supplementary Fig. S3*C*). These data may indicate that activated Akt1 enhances the cytotoxic side effect(s) of vanadate or negatively regulates the suppressive effect of vanadate.

To ascertain whether vanadate or PFTα suppressed p53-independent mitochondrial dysfunction, we investigated their effects on the anisomycin-induced loss of $\Delta\psi$m and on the apoptosis induced by expressing exogenous Bax (Supplementary Fig. S3*D*). Anisomycin was used to stimulate c-Jun NH_2-terminal kinase–dependent apoptosis (12, 29), and Bax as a direct activator of mitochondrial apoptosis (30). Neither vanadate nor PFTα protected the cells from these p53-independent mitochondrial-dependent apoptotic pathways. These data also indicate that neither of these agents is a general inhibitor of mitochondrial apoptosis.

Vanadate suppresses p53-dependent mitochondrial apoptotic events, but PFTα does not. We further investigated the effects of vanadate and PFTα on mitochondrial apoptotic events, that is, the loss of $\Delta\psi$m and the conformational changes of Bax and Bak (12, 31, 32). We found that these events were p53 dependent using p53-knockdown transformants (Supplementary Fig. S4). The suppression of the $\Delta\psi$m loss by vanadate was dose dependent, whereas PFTα was ineffective against the loss and showed potent mitochondrial toxicity at 80 μmol/L (Fig. 3*A*). [Because PFTα fully inhibited p53-induced transcription at 50 μmol/L (Fig. 2*A*) and was not toxic at this concentration, we used it at 50 μmol/L in the following experiments.] We obtained similar results for the conformational change of Bax and Bak (Fig. 3*B* and *C*). Of note, because the loss of $\Delta\psi$m was low 6 hours after IR (12), we measured it 12 hours after IR, whereas Bax and Bak were activated 6 hours after IR. These results suggest that, in irradiated MOLT-4 cells, the activation of Bax and Bak may precede the loss of $\Delta\psi$m, which may not follow immediately. These results were consistent with the ineffectiveness of PFTα against the radiation-induced apoptosis of MOLT-4 cells and indicated that vanadate, but not PFTα, suppresses p53-driven transcription-independent mitochondrial apoptotic events. Therefore, we next investigated the effects of PFTμ on the apoptosis. The suppressive effect of PFTμ exceeded that of PFTα and was slightly less than that of vanadate; the combined treatment with PFTμ and PFTα was not much greater than that of PFTμ alone (Fig. 3*D*). These data indicated that the transcription-independent p53 pathway is predominant in irradiated MOLT-4 cells. In addition, because PFTμ at 10 μmol/L showed a marked inhibitory effect on the transactivation of PUMA, we used it at 7.5 μmol/L in the following experiments.

Vanadate suppresses the transcription-independent pathway. We next investigated the effect of vanadate on the transcription-independent p53 pathway in irradiated MOLT-4 cells. First, we analyzed its effects on the translocation of p53 to mitochondria, a key initial event in this pathway (13–17), in fractionated MOLT-4 cells. Subcellular fraction 1 contained mitochondria and membrane organelles, including ER, and fraction 2 contained cytosolic components, as assessed by several marker proteins (Fig. 4*A*). In fractionated, irradiated MOLT-4 cells, vanadate treatment caused substantial reduction of the post-IR p53 in fraction 1, and PFTμ had a moderate effect, but neither altered the amount of p53 in fraction 2. Because p53 was present even in fraction 1 samples that contained little ER, p53 seemed to be predominantly located at the mitochondria. Vanadate and PFTμ also suppressed the interaction—essential for the direct initiation of apoptosis—of p53 with Bcl-2 (Fig. 4*B*). We also investigated the ability of p53 to bind two other known interaction partners, Bcl-xL and Bak; however, these interactions were weak in irradiated MOLT-4 cells and therefore unlikely to be important for this form of apoptosis (data not shown). Collectively,

these data indicate that vanadate and PFTμ suppress the transcription-independent apoptotic events in irradiated MOLT-4 cells, and PFTα (at least at 50 μmol/L) does not.

Vanadate suppresses the apoptosis-inducing activity of mitochondrially targeted ts p53. To further characterize the effects of vanadate on transcription-independent p53-mediated apoptosis, we used p53-null SaOS-2 cells to establish stable transfectants expressing one of two forms of ts p53s: Lp53 (a mitochondrially targeted ts p53) and Np53 (originally Nucl p53; a nucleus-directed ts p53; refs. 13, 14, 21). In this system, these temperature-shifted ts p53–expressing cells predominantly undergo growth retardation, but a fraction of them die through apoptosis. Np53 is largely translocated to the nucleus at the permissive temperature (30°C; ref. 14), although some extranuclear Np53 remains, including at mitochondria (21). The localizations of Lp53 and Np53 were analyzed by immunofluorescence staining (Supplementary Fig. S5).

We quantified the transcriptional activity of the temperature-shifted Np53 using a sensitive p53 reporter assay and found an ~500-fold induction relative to the level at the nonpermissive temperature (Fig. 5*A*). In contrast, Lp53 caused only a 3-fold induction, which was reasonable because its transcriptional activity is impaired (14); concordantly, Lp53 did not induce MDM2 and p21 (Fig. 5*B*). To verify that Lp53 was imported into mitochondria, we used immunoblotting to detect cleavage of the mitochondrial import leader peptide, which is fused to Lp53 and cleaved only by the endogenous mitochondrial endopeptidase (Fig. 5*B*).

We next investigated the expression of the apoptosis-related Bax, PUMA, active caspase-3 and caspase-7, MDM2, and p21 in the Np53- and Lp53-expressing cells. MDM2 and p21 were upregulated by the temperature shift, and the upregulation was suppressed substantially by vanadate (200 μmol/L) and moderately by PFTα (80 μmol/L). Although few changes in Np53 expression were observed after the temperature shift in the vanadate- and PFTα-treated cells, presumably due to its already robust expression, a slight increase observed in the vanadate-treated cells might have been related to the suppression of MDM2 induction. Bax was not upregulated in the temperature-shifted Np53- or Lp53-expressing cells (Fig. 5*B*), and PUMA was not detected in the cells at all (data not shown), but both ts p53s induced caspase activation after the temperature shift. Thus, Lp53 is an excellent initiator of the transcription-independent pathway, and we used Np53 as a control for the normal p53 pathways, including the transcription-dependent pathway. Vanadate suppressed the caspase activation by both ts p53s, whereas PFTα did not suppress the Lp53-induced but substantially inhibited the Np53-induced caspase activation. The effects of PFTμ on caspase activation were the opposite of the effects of PFTα. The corresponding apoptotic

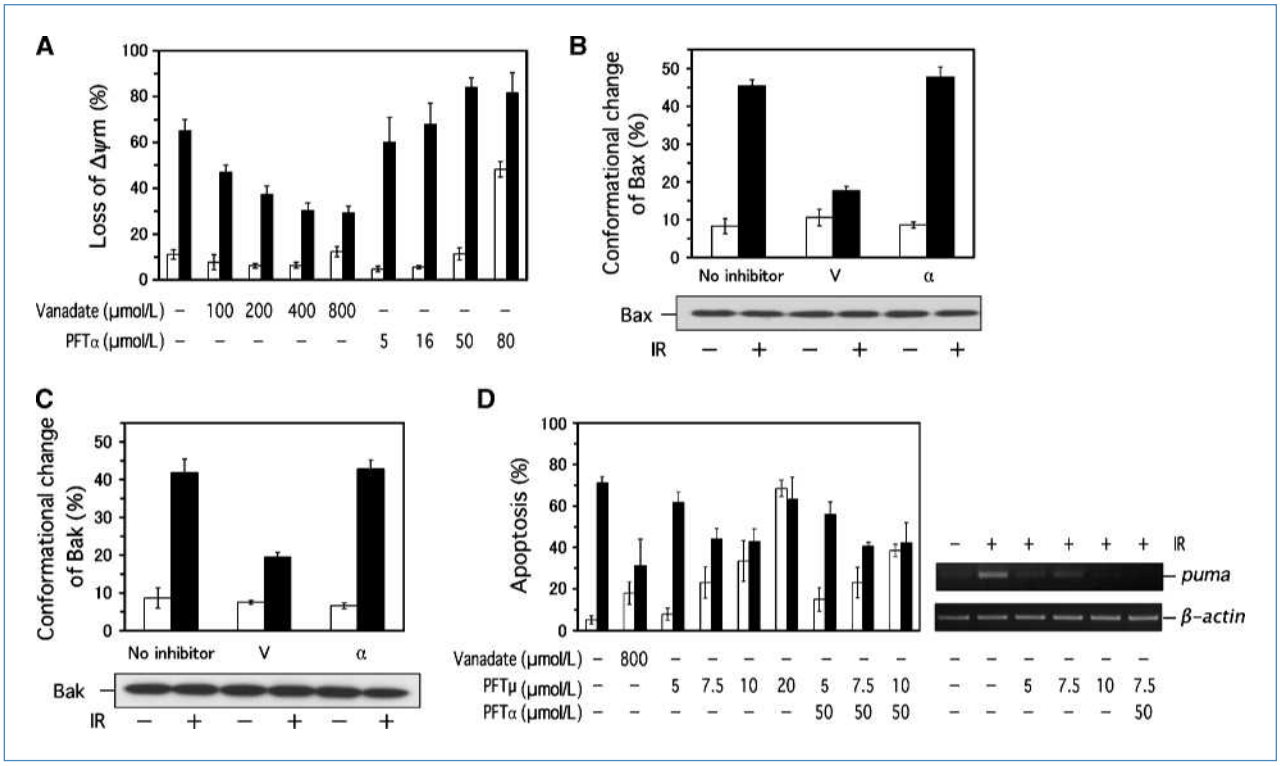

Figure 3. Vanadate suppresses the Δψm loss and Bax and Bak conformational change in irradiated MOLT-4 cells, but PFTα does not. *White columns,* unirradiated samples; *black columns,* 10 Gy–irradiated samples. *Columns,* mean ($n \geq 3$); *bars,* SD. *A,* flow cytometric analysis of Δψm loss (12 h after treatment). *B* and *C,* flow cytometric analysis of Bax and Bak conformational change (6 h after treatment). *Bottom,* immunoblots with the same antibodies used in the flow cytometric analysis. Vanadate (*V*) was used at 800 μmol/L, and PFTα (*α*) at 50 μmol/L. *D,* PFTμ, inhibitor of the transcription-independent pathway, suppressed apoptosis in 10 Gy–irradiated MOLT-4 cells. Apoptotic cells were quantified by Annexin V-FITC staining 18 h after treatment. *Right,* RT-PCR analysis of *puma* transcription (6 h after treatment).

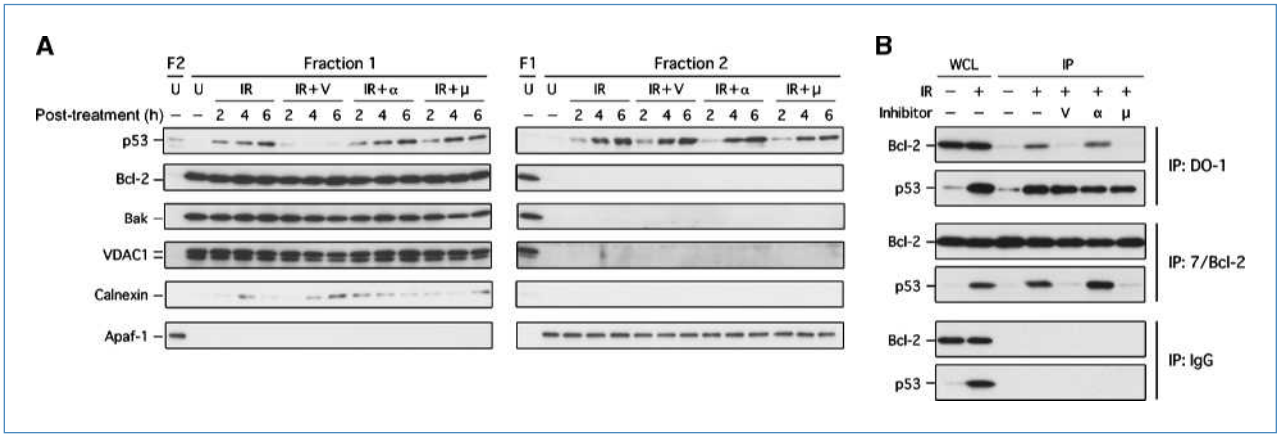

Figure 4. Vanadate interferes with the mitochondrial translocation of p53. Vanadate, PFTα, and PFTμ (*μ*) were at 800, 50, and 7.5 μmol/L, respectively. *IR,* 10 Gy. *A,* the fractions were isolated at the indicated times after treatment. Proteins were detected by immunoblotting. *F1,* fraction 1; *F2,* fraction 2; *U,* unirradiated control; *Bcl-2, Bak,* and *VDAC1,* mitochondrial markers; *Calnexin,* ER marker; *Apaf-1,* cytosolic marker. *B,* immunoprecipitation of Bcl-2 and p53 in irradiated MOLT-4 cells (6 h after IR). Whole-cell lysates (*WCL*) from unirradiated (*lane 1*) or 10 Gy–irradiated (*lane 2*) MOLT-4 cells cultured for 6 h were the negative and positive controls, respectively, for p53. They were also used as positive controls for Bcl-2.

rates are shown in Fig. 5*C*. Thus, PFTα is a poor inhibitor of the transcription-independent pathway, and PFTμ is a poor inhibitor of the transcription-dependent pathway.

We also assessed the effects of these p53 inhibitors on the interaction between the temperature-shifted Np53 and Bcl-2 (Fig. 5*D*). Vanadate reduced the binding to below the level at the nonpermissive temperature. PFTμ partially suppressed the binding, and PFTα did not affect it. Collectively, these findings showed that vanadate potently suppresses the transcription-independent pathway.

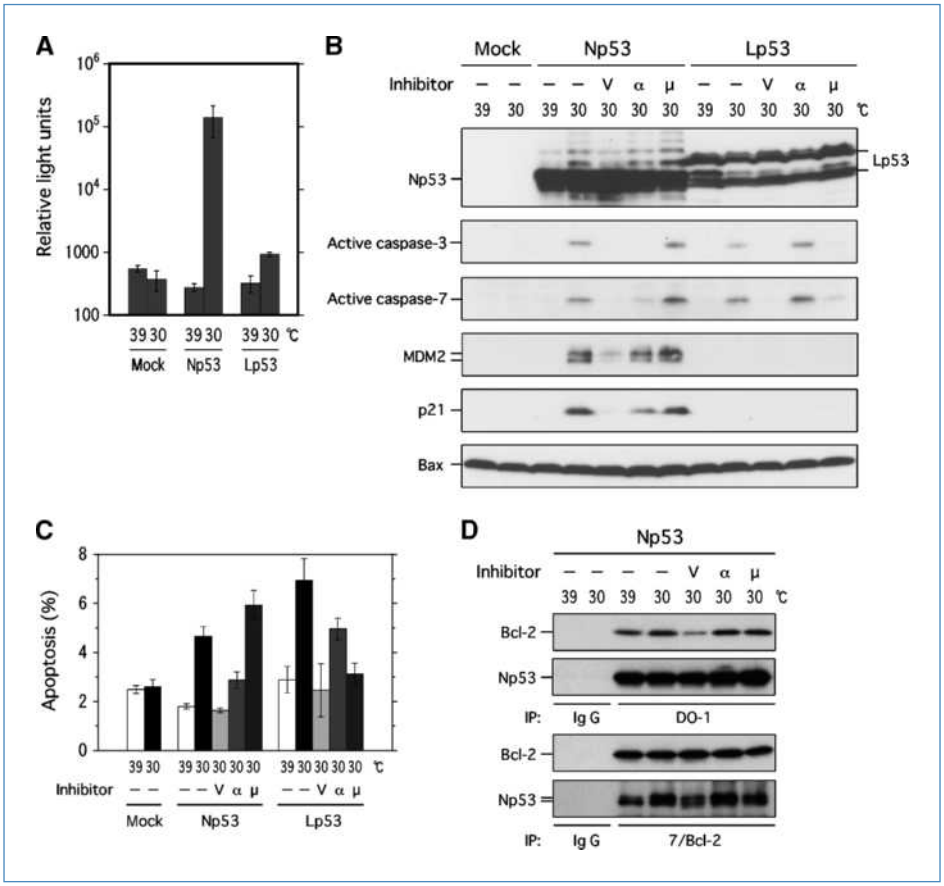

Figure 5. Vanadate suppresses the apoptosis-inducing activity of mitochondrially targeted ts p53. SaOS-2 stable transfectants were incubated with or without p53 inhibitors and kept at 39°C or 30°C for 24 h. Vanadate, PFTα, and PFTμ were at 200, 80, and 7.5 μmol/L, respectively. *Columns,* mean ($n \geq 3$); *bars,* SD. *A,* SaOS-2 stable transfectants transiently expressing the p53-Luc plasmid and carrier DNA (pcDNA3.1; 1:4 mixture) were incubated at 39°C for 3 h and then shifted to the optimal permissive temperature (30°C) for 24 h. *B,* effect of p53 inhibitors on Np53- or Lp53-induced caspase activation at the permissive temperature. Proteins were detected by immunoblotting. *C,* apoptotic rate was determined by Poly-Caspases FLICA Apoptosis Detection kit (ICT). *D,* immunocoprecipitation of Bcl-2 and Np53.

Vanadate has potent radioprotective activity against both gastrointestinal and hematopoietic syndrome. Although vanadate was superior to PFTα in suppressing p53-dependent apoptosis, especially in the transcription-independent pathway, a radioprotective effect of PFTα in mice has already been shown (5). We did not find a radioprotective effect of PFTμ in either ICR or C57BL/6J mice (data not shown). To avoid potentially confounding side effects from the cytotoxicity of PFTα, we chose cPFTα as an equivalent alternative, as a reference for vanadate in our mouse study. We used 8 and 12 Gy of total body IR (TBI), which induce, respectively, hematopoietic and gastrointestinal syndrome in ICR mice (33–36). For the i.p. administrations, we used 20 mg/kg cPFTα and vanadate. This concentration of cPFTα was a dose determined in previous studies and our pilot study as double the requirement for PFTα to suppress the hematopoietic syndrome (5). The dosage of vanadate was approximately one third its LD_{50} value, as assessed in our pilot study, when delivered i.p. into mice, and was similar to the dose used in wild-type p53 thymocytes (Supplementary Fig. S2*C*). No abnormal behavior and no lethality (Supplementary Fig. S6*A*) were observed at this dose of cPFTα or vanadate.

Both treatments protected the mice from a sublethal dose of 8 Gy TBI, which killed two thirds of the control (physiologic saline injected) mice (Fig. 6*A*), and there was no significant difference between the vanadate- and cPFTα-treated subgroups. Vanadate rescued 60% of the mice treated with 12 Gy TBI, which killed all of the control mice within 12 days, but cPFTα did not protect them at this lethal dose, as reported for PFTα (5). The protective effect of vanadate at 12 Gy TBI was significantly greater than that of cPFTα ($P < 0.0002$). We also tested the protective effects of vanadate using a supralethal

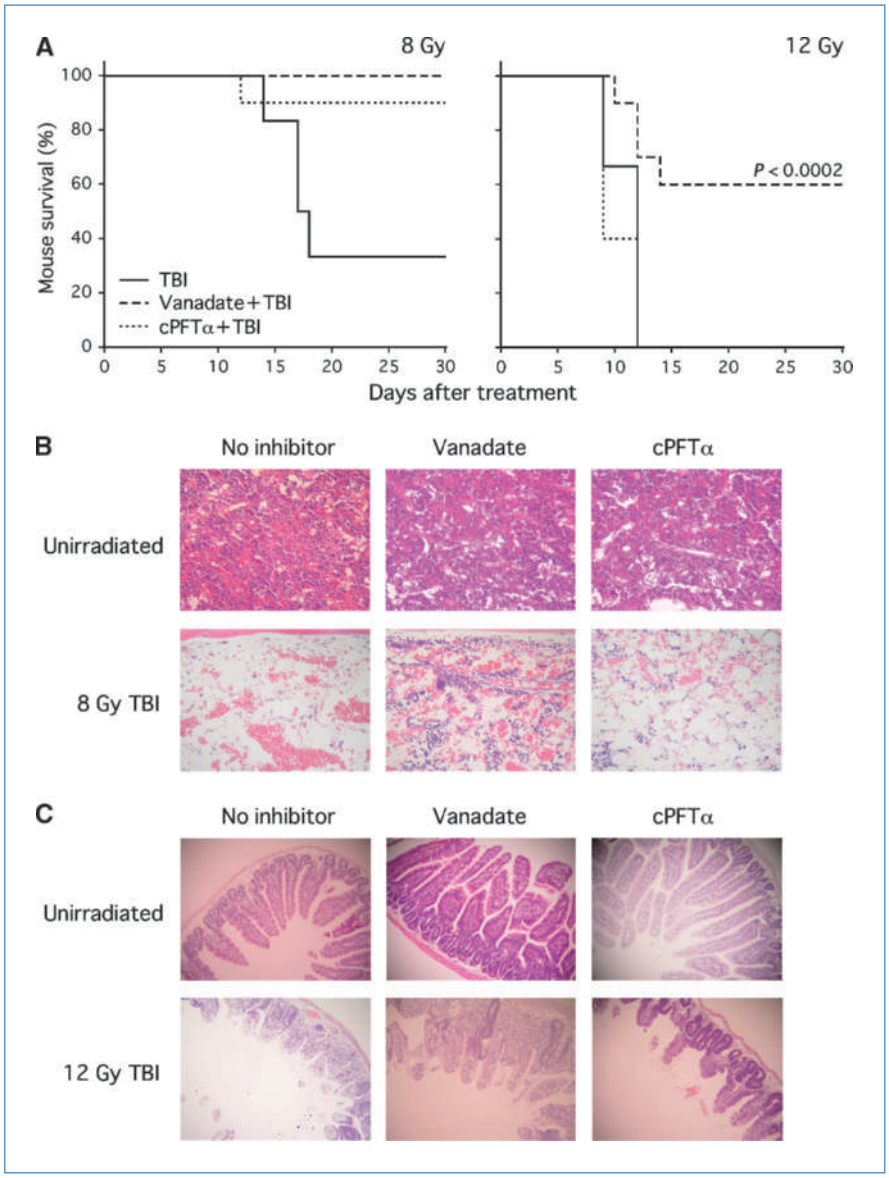

Figure 6. Vanadate protects irradiated mice from dying of either gastrointestinal or hematopoietic syndrome. *A,* 30-d survival tests of ICR mice after 8 or 12 Gy of TBI. Ten mice were used in each experimental subgroup, except for the subgroups of 8 Gy TBI alone (6 mice) and 12 Gy TBI alone (3 mice). *P,* comparison between the vanadate-treated and the cPFTα-treated subgroups (Student's *t* test). *B* and *C,* radioprotective efficacies of vanadate and cPFTα in H&E-stained sections of target tissues. The femurs were observed 7 d after 8 Gy TBI (*B*, ×300 magnification), and the intestine was observed 4 d after 12 Gy TBI (*C*, ×150 magnification).

dose of 13 Gy TBI (Supplementary Fig. S6*B*). Although the vanadate treatment did not rescue these mice, there was a trend toward prolonged survival, but it was observed only in 2 of 10 mice. Thus, the dose reduction factor (the fold change in IR dose to produce a given level of lethality) for vanadate was estimated to be 1.5 to 1.6, which is good compared with other radioprotectors (1, 3, 35, 36).

Finally, we performed a pathologic study on the bone marrow of femurs and the small intestine and showed that vanadate efficiently inhibited the reduction of bone marrow cells (bone marrow aplasia) and relieved the epithelial damage (disappearance of crypts and shortening of villi) more effectively than cPFTα (Fig. 6*B* and *C*), indicating strong correlations with the survival results. The transcriptional inhibitory effects of them were confirmed by RT-PCR analysis (Supplementary Fig. S6*C*).

Discussion

Building on the results of our previous study (12), here we showed that vanadate is a bifunctional inhibitor of p53 that suppresses both its transcription-dependent and transcription-independent pathways. Our data suggest that inhibition of both p53 pathways is a more potent antiapoptotic strategy than inhibition of one of them, which is supported by the limited efficacies of the single-pathway inhibitors PFTα and PFTμ (5, 6) versus vanadate.

One study showed that p53-knockout mice are protected from hematopoietic syndrome–induced death but shows heightened lethality from gastrointestinal syndrome (5). These results were explained by the severe impairment of p21–mediated growth arrest that presumably gave the damaged cells some recovery time. The difference in gastrointestinal sensitivity between the genetic approach and the pharmacologic inhibition used here was probably owing to the constitutive lack of p53 function in the knockout mice, which is only temporarily inhibited pharmacologically; in our pilot study, a single i.p. injection of vanadate 2 hours before 12 Gy TBI did not show any protective activity (data not shown). The key to safe radioprotection is the short-term inhibition of p53. This is evidenced by the resistance to radiation–induced tumorigenesis when p53 is transiently inactivated during the acute radiation response in genetically engineered mice, by the finding that PFTα and cPFTα do not increase the lethality from gastrointestinal syndrome, and by the observation that vanadate protects 12 Gy–irradiated mice from death (Fig. 6; refs. 5, 9). It is possible that part of the radioprotection is mediated by the function of p53 as an inhibitor of mitotic catastrophe, which might recover from the pharmacologic inhibition before the radiation injury becomes irreversible.

In irradiated MOLT-4 cells, neither PFTα nor salicylate suppressed apoptosis despite their suppression of p53-dependent transcription, indicating that this apoptosis does not require p53-dependent transcription. The suppression of apoptosis by PFTμ in the cells strengthens this idea. Thus, MOLT-4 apoptosis is a useful system for studying the transcription-independent pathway. Alternatively, the transcriptional inhibition of p53 might augment the transcription-independent pathway. Such augmentation by PFTα was recently reported in chronic lymphocytic leukemia cells (37).

Although vanadate has an antiapoptotic advantage in suppressing both pathways, it did not completely suppress the lethality of gastrointestinal syndrome. We do not regard this as a practical limit for radioprotection through the suppression of both pathways because vanadate has a dose-limiting toxicity, and the bioavailable dose in mice is substantially lower than that in cultured cells. A less toxic compound capable of suppressing both pathways may serve as a therapeutic inhibitor of p53.

Disclosure of Potential Conflicts of Interest

No potential conflicts of interest were disclosed.

Grant Support

Grant-in-Aid for Young Scientists (B) from the Japan Society for the Promotion of Science, Grants from the Radiation Effects Association (Japan), and the Public Trust Haraguchi Memorial Cancer Research Fund (A. Morita).

The costs of publication of this article were defrayed in part by the payment of page charges. This article must therefore be hereby marked *advertisement* in accordance with 18 U.S.C. Section 1734 solely to indicate this fact.

Received 9/30/08; revised 10/16/09; accepted 10/22/09; published online 1/4/10.

References

1. Hall EJ, Giaccia AJ. Radiobiology for the radiologist. 6th ed. pp. 117–34 Philadelphia: Lippincott Williams & Wilkins; 2006.
2. Dodd MJ. Managing the side effects of chemotherapy and radiation. San Francisco: UCSF Nursing Press; 2001.
3. Weiss JF, Landauer MR. Protection against ionizing radiation by antioxidant nutrients and phytochemicals. Toxicology 2003;189:1–20.
4. Komarov PG, Komarova EA, Kondratov RV, et al. A chemical inhibitor of p53 that protects mice from the side effects of cancer therapy. Science 1999;285:1733–7.
5. Komarova EA, Kondratov RV, Wang KH, et al. Dual effect of p53 on radiation sensitivity *in vivo*: p53 promotes hematopoietic injury, but protects from gastro-intestinal syndrome in mice. Oncogene 2004; 23:3265–71.
6. Strom E, Sathe S, Komarov PG, et al. Small-molecule inhibitor of p53 binding to mitochondria protects mice from γ radiation. Nat Chem Biol 2006;2:474–9.
7. Sugioka R, Shimizu S, Funatsu T, et al. BH4-domain peptide from Bcl-x(L) exerts anti-apoptotic activity *in vivo*. Oncogene 2003;22: 8432–40.
8. Burdelya LG, Krivokrysenko VI, Tallant TC, et al. An agonist of toll-like receptor 5 has radioprotective activity in mouse and primate models. Science 2008;320:226–30.
9. Christophorou MA, Ringshausen I, Finch AJ, Swigart LB, Evan GI. The pathological response to DNA damage does not contribute to p53-mediated tumour suppression. Nature 2006;443:214–7.
10. Chernov MV, Stark GR. The p53 activation and apoptosis induced by DNA damage are reversibly inhibited by salicylate. Oncogene 1997; 14:2503–10.

11. Meplan C, Mann K, Hainaut P. Cadmium induces conformational modifications of wild-type p53 and suppresses p53 response to DNA damage in cultured cells. J Biol Chem 1999;274:31663–70.
12. Morita A, Zhu J, Suzuki N, et al. Sodium orthovanadate suppresses DNA damage-induced caspase activation and apoptosis by inactivating p53. Cell Death Differ 2006;13:499–511.
13. Marchenko ND, Zaika A, Moll UM. Death signal-induced localization of p53 protein to mitochondria—a potential role in apoptotic signaling. J Biol Chem 2000;275:16202–12.
14. Mihara M, Erster S, Zaika A, et al. p53 has a direct apoptogenic role at the mitochondria. Mol Cell 2003;11:577–90.
15. Chipuk JE, Kuwana T, Bouchier-Hayes L, et al. Direct activation of Bax by p53 mediates mitochondrial membrane permeabilization and apoptosis. Science 2004;303:1010–4.
16. Leu JIJ, Dumont P, Hafey M, Murphy ME, George DL. Mitochondrial p53 activates Bak and causes disruption of a Bak-Mcl1 complex. Nat Cell Biol 2004;6:443–50.
17. Marchenko ND, Wolff S, Erster S, Becker K, Moll UM. Monoubiquitylation promotes mitochondrial p53 translocation. EMBO J 2007;26: 923–34.
18. Bonini P, Cicconi S, Cardinale A, et al. Oxidative stress induces p53-mediated apoptosis in glia: p53 transcription-independent way to die. J Neurosci Res 2004;75:83–95.
19. Arima Y, Nitta M, Kuninaka S, et al. Transcriptional blockade induces p53-dependent apoptosis associated with translocation of p53 to mitochondria. J Biol Chem 2005;280:19166–76.
20. Horton RM. *In vitro* recombination and mutagenesis of DNA. SOEing together tailor-made genes. In: White BA, editor. PCR cloning protocols. From molecular cloning to genetic engineering. New Jersey: Humana Press; 1997, p. 141–9.
21. Dumont P, Leu JIJ, Della Pietra AC, George DL, Murphy M. The codon 72 polymorphic variants of p53 have markedly different apoptotic potential. Nat Genet 2003;33:357–65.
22. Rocha S, Campbell KJ, Roche KC, Perkins ND. The p53-inhibitor pifithrin-α inhibits firefly luciferase activity *in vivo* and *in vitro*. BMC Mol Biol 2003;4.
23. Burdelya LG, Komarova EA, Hill JE, et al. Inhibition of p53 response in tumor stroma improves efficacy of anticancer treatment by increasing antiangiogenic effects of chemotherapy and radiotherapy in mice. Cancer Res 2006;66:9356–61.
24. Wei Q. Pitx2a binds to human papillomavirus type 18 E6 protein and inhibits E6-mediated p53 degradation in HeLa cells. J Biol Chem 2005;280:37790–97.
25. Jia LQ, Osada M, Ishioka C, et al. Screening the p53 status of human cell lines using a yeast functional assay. Mol Carcinogen 1997;19: 243–53.
26. Cheng J, Haas M. Frequent mutations in the p53 tumor suppressor gene in human leukemia T-cell lines. Mol Cell Biol 1990;10:5502–09.
27. Murai Y, Hayashi S, Takahashi H, Tsuneyama K, Takano Y. Correlation between DNA alterations and p53 and p16 protein expression in cancer cell lines. Pathol Res Pract 2005;201:109–15.
28. Bozulic L, Surucu B, Hynx D, Hemmings BA. PKBα/Akt1 acts downstream of DNA-PK in the DNA double-strand break response and promotes survival. Mol Cell 2008;30:203–13.
29. Enomoto A, Suzuki N, Kang Y, et al. Decreased c-Myc expression and its involvement in X-ray-induced apoptotic cell death of human T-cell leukaemia cell line MOLT-4. Int J Radiat Biol 2003; 79:589–600.
30. Jurgensmeier JM, Xie ZH, Deveraux Q, Ellerby L, Bredesen D, Reed JC. Bax directly induces release of cytochrome *c* from isolated mitochondria. Proc Natl Acad Sci U S A 1998;95:4997–5002.
31. Roucou X, Martinou JC. Conformational change of Bax: a question of life or death. Cell Death Differ 2001;8:875–7.
32. Desagher S, Osen-Sand A, Nichols A, et al. Bid-induced conformational change of Bax is responsible for mitochondrial cytochrome *c* release during apoptosis. J Cell Biol 1999;144:891–901.
33. Lei M, Wang JF, Wang YM, et al. Study of the radio-protective effect of cuttlefish ink on hemopoietic injury. Asia Pac J Clin Nutr 2007;16: 239–43.
34. Kim SG, Nam SY, Kim CW. *In vivo* radioprotective effects of oltipraz in γ-irradiated mice. Biochem Pharmacol 1998;55:1585–90.
35. Mantena SK, Unnikrishnan MK, Joshi R, Radha V, Devi PU, Mukherjee T. *In vivo* radioprotection by 5-aminosalicylic acid. Mutat Res 2008; 650:63–79.
36. Baliga MS, Jagetia GC, Venkatesh P, Reddy R, Ulloor JN. Radioprotective effect of abana, a polyherbal drug following total body irradiation. Br J Radiol 2004;77:1027–35.
37. Steele AJ, Prentice AG, Hoffbrand AV, et al. p53-mediated apoptosis of CLL cells: evidence for a transcription-independent mechanism. Blood 2008;112:3827–34.